AD 740863

CHARACTERIZATION OF PARTICULATE CERAMIC MATERIALS BY COMPUTERIZED SCANNING ELECTRON MICROSCOPE TECHNIQUES

E. W. White, H. A. McKinstry
and G. G. Johnson, Jr.

DDC
APR 27 1972

Final Report

Office of Naval Research, Metallurgy Program
Contract No. N00014-67-A-0385-0007

31 March 1972

Reproduced by
NATIONAL TECHNICAL
INFORMATION SERVICE
Springfield, Va 22151

DISTRIBUTION STATEMENT A
Approved for public release;
Distribution Unlimited

DISTRIBUTION OF THIS DOCUMENT IS UNLIMITED: REPRODUCTION IN WHOLE OR IN PART IS PERMITTED FOR ANY PURPOSE OF THE UNITED STATES GOVERNMENT.

THE MATERIALS RESEARCH LABORATORY

THE PENNSYLVANIA STATE UNIVERSITY

UNIVERSITY PARK, PENNSYLVANIA

45

LIST OF PERSONNEL SUPPORTED BY THIS CONTRACT

In addition to the principal investigators, the following personnel have been supported by this program for some interval. Where graduate research has led to completion of a thesis, degrees granted are indicated in parentheses:

Dr. H. Görz

Mr. R. Hoover

Mr. J. Lebiedzik (M.S.: Solid State Science)

Mr. W.L. Matson (M.S.: Computer Science)

Miss K. Mayberry (M.S.: Computer Science)

Mr. R.E. McMillan (M.S.: Computer Science)

Miss M. Pearson (M.S.: Computer Science)

Details of illustrations in this document may be better studied on microfiche

TABLE OF CONTENTS

LIST OF TABLES

LIST OF FIGURES

ABSTRACT

During this three-year program, techniques have been developed for the quantitative characterization of particulate materials by computer evaluation of scanning electron microscope images (CESEMI). The full CESEMI analysis is particularily applicable to particles in the size range of 0.1 to 100μm diameter. It measures, particle-by-particle, the following basic parameters: 1) projected area, 2) perimeter, 3) major axis of fitted ellipse, 4) minor axis of fitted ellipse, 5) orientation of major axis and 6) particle type as deduced from characteristic x-ray signals for the elements. The computer routinely presents plots of both the basic and derived parameters (A/P^2, probability versus log of equivalent circular diameter, etc.).

Sample preparation is often a major limitation to particulate characterization. A new method has been developed that is especially well suited for dispersing ceramic raw materials for SEM work. The eutectic composition of camphor and naphthalene is an ideal dispersing medium as it can be handled as a solid or viscous liquid. Also, it completely sublimes in modest vacuum, leaving no confusing residue to complicate the SEM images.

CESEMI analysis has been extended to some applications of quantitative petrography and is applicable to certain types of surface finish analysis.

In addition to detailed CESEMI analyses, some very simple forms of quantitative image analysis have been instrumented. These are simple point-counting by electronic scalers and direct accumulation of chord-length distribution. These simple methods, although quite quantitative, have a limited interpretation in that the real shapes of particles cannot be taken into account. Nevertheless, these analyses are very simple to execute and have proven very useful in analyses of many powders and in petrographic analysis--especially of porosity.

Both the full CESEMI analysis and the simple techniques can now be used routinely. We look forward to applying these techniques to a wide variety of materials processing problems. Because CESEMI has been the subject of several reports and publications, the technique is not described in detail in this report. On the other hand, the simple image analysis procedures have been only recently developed and are described in detail for the first time.

I. INTRODUCTION

This research program was begun just three years ago to develop methods for the computer evaluation of scanning electron microscope images (CESEMI) and to apply these methods to the quantitative characterization of selected particulate aluminas. CESEMI methods developed not only apply to the quantitative characterization of aluminas but to particulate samples in general. In one variation of this method, multi-phase powders are characterized in such a way that the characteristics of each chemically different phase are computed without having to mechanically separate the phases. Also, developed are techniques for quantitative petrography and surface finish analysis.

Because the full CESEMI analysis may not be required in many applications, we have developed, in parallel, simple techniques for point counting and lineal analysis that do not require sophisticated computer programs Rather, point count and lineal analysis data are collected rapidly by scalers or multichannel analyser. This approach has proved useful in rapid evaluation of pore characteristics as well as in comparison of particulate samples.

The basic techniques developed in this program are proving to be useful in the characterization of a wide variety of materials. Particularly interesting "spin-offs" have been in the analysis of airborne particulates, coal mine dusts and metal powders.

II. GENERAL APPROACH TO CHARACTERIZATION

The multitude of signals generated by electrons bombarding a solid target provide the most versatile single instrument capability for materials characterization. In the conventional scanning electron microscope (SEM), for example, a rastered, finely-focused electron beam (100Å diameter) generates a secondary electron signal that produces a high resolution (150Å), large depth of field image of the surface topography. As a result of the quality of the images and the ease of specimen preparation, the SEM is now employed in a wide range of materials problems. In the more familiar electron microprobe instrument, the characteristic x-ray signals are detected to yield micron scale elemental chemical analyses of all elements except hydrogen, helium, lithium and beryllium. As SEM technology has advanced, there has been a tendency to combine the SEM and electron microprobe capabilities into one instrument. We will consider the combined SEM-electron probe instrumentation throughout this discussion.

Several of the more important kinds of signals are tabulated in Table I. It is important to realize that all these signals are generated simultaneously, whether or not they are of interest or used in a given experiment. Table I is constructed assuming typical operating conditions of 150Å electron beam diameter, operating at 25 kev and specimen current on the order of 10^{-10} amps. The best spatial resolution is realized in the secondary electron images while the lowest resolution is observed in x-ray and cathodoluminescence images. This poorer resolution results from the large volume range of primary electrons that generate these signals.

The method of image formation in a SEM or probe is particularly well suited to quantitative image analysis. Unlike light or transmission electron microscopy, where the entire image is generated and available simultaneously, the SEM generates an image bit-by-bit in a systematic and piece-meal manner. As the finely focused electron beam sweeps across the specimen surface, the emission intensity of one of the signals (secondary electron emission, for example) is instantaneously monitored and the signal level is used to modulate the brightness

TABLE I. CONTRAST MECHANISMS IN THE SEM.

	Signal	Features Imaged	Typical* Resolution	Sampling* Time per Picture Point (sec.)
1.	Secondary Electron	Surface Topography	150Å	10^{-5}
2.	Absorbed Electron Current	Average Atomic Number on Smooth Flat Surfaces. Topography of Rough Surfaces.	1000Å	10^{-4}
3.	Electron Backscatter	Average Atomic Number on Smooth Flat Surfaces. Topography of Rough Surfaces.	1000Å	10^{-5}
4.	Auger Electrons	Surface Chemistry (50Å depth) Most Suitable for Lighter Elements (B → Cl).	0.5→10μm	1
5.	Characteristic X-ray	Elemental Chemical Analysis. Readily Resolves Adjacent Elements. Handles All Elements Boron and Heavier in Minor and Major Concentrations.	1→10μm	10^{-4} - 10
6.	Continuum X-ray	Rarely a Useful Signal. Contributes Background Noise to Characteristic X-ray Signals.	1→10μm	1 - 10
7.	Cathodoluminescence	Most Non-metallic Materials Exhibit C.L. to Some Degree.	1→10μm	10^{-5} -10^{-3}
8.	Voltage Contrast	Potential Gradients on Surface (Voltage Differences on the Order of 10 mV Have Been Resolved.).	1→10μm	10^{-5}

* Values are meant merely to indicate approximate figures with due respect to variations arising from special effort or select conditions.

of the display cathode ray tube (CRT). If the beam on the CRT is made to sweep out a square frame in a series of lines (really analogous to the motion of one's eyes in reading the lines on this page), and if the motion of the electron beam on the display screen is coupled synchronously, then a coherent image appears on the display.

The following points highlight the important aspects to our approach to image analyses:

1. The image frame (picture) is decomposed into a matrix of picture points. Picture point densities vary from 256 points per line to 1024 points per line. Higher densities (4096 points per line) are being considered in newer versions of the instrument.

2. Image information can be monitored directly, electronically, independent of any visual display. This is an extremely important feature of this work since the electron beam on the sample can be controlled to a greater accuracy than the CRT displays. Also, the beam on the sample can be made to sweep with a greater resolution than can be achieved in the existing CRT displays.

3. The electron beam in the SEM is controlled by a digital sweep generator such that the dwell-time on a given image point can be precisely controlled and adjusted over a wide range. This facilitates collection of all signals of interest simultaneously at a given picture point with no image overlay error that would result from working with a separate sweep for each signal of interest.

4. The scanning electron microscope carries several advantages over a light microscope, for example, in that it functions with a high depth of field (some 300 times greater than for a light microscope at a given magnification setting) thus making it quite easy to resolve large or small particles in a given field without having to adjust the focus.

5. The resolution and magnification range of the SEM is such that one can work readily with particles over the size range from 0.1 to 100 μm. This allows one to cover the size range of most particulate

materials with one instrument.

6. In the CESEMI work, entire images are handled in the computer to render measurements independent of raster orientation. Two basic program approaches have been developed: 1) the contour method and, 2) the binary, coded-map method.

III. SAMPLE PREPARATION

In any analysis of particulate samples, the results are no better than the quality of preparation or the validity of sampling. For the best analysis, each particle should be isolated and measured independent of all other particles. For the SEM, the particles should be dispersed on a featureless substrate. We have spent a great deal of work on developing techniques for dispersion as well as in preparing substrates for the various applications.

A. Camphor-Naphthalene Dispersion Technique

The method that has been developed for dispersing samples involves the use of an eutectic composition of camphor and naphthalene. This technique is described in detail in our Technical Report No. Five[1], and will appear soon in "Powder Technology".

The camphor-naphthalene eutectic composition (60 wt % camphor) is an ideal dispersing medium in that it can be manipulated either as a soft crystalline solid or as a liquid of variable viscosity merely by changing its temperature over the range from about 28 to 40°C (melting point = 32°C).

The general preparation procedure involves cutting a portion of the stock eutectic solution and heat-sealing it together with a known amount of the particulate sample in a polyethylene bag. The specimen can be dispersed by kneeding it while in the sealed bag. When mixing is carried out, the mixture is chilled to a solid to "freeze-in" the dispersion. Contents of the bag can be sampled without biasing the characteristics of the remainder. A portion of the blended material is transferred as a solid to the substrate surface and gently melted under a glass cover slip. As soon as the sample has spread to a uniformally thin layer under the cover slip, the substrate is quickly chilled to freeze the eutectic medium. The cover slip is pried off and the substrate with sample is transferred to a vacuum chamber and evacuated to about 10-20 Torr

for 20-30 minutes. During this time, the eutectic completely sublimes leaving only the dispersed particles on the substrate. For conductive substrates, no conductive coating is used but for glass substrates; i. e. it is necessary to apply a coating such as 200Å of gold.

This technique has been used to prepare a wide variety of particulate materials including alumina, Portland cement, ferrite, coal dust, tungsten and tantalum metal powders and several inorganic phosphors.

B. Substrates

A variety of substrates have been perfected. Each has its particular advantage depending on the particular study.

1. The simplest material is a common glass microscope slide which is given a light gold coat (~200Å) after the dispersion is made. Carbon coating does not yield as featureless a substrate as does the gold and contrast of particle to background is not as favorable for carbon.

2. Carefully polished beryllium, although difficult to prepare, affords the best substrate when one wishes to distinguish particles chemically based on characteristic x-ray emission. In addition to having no interfering x-ray lines, its continuum emission is very low, and it, of course, requires no conductive coating. Secondary electron image contrast for particles on beryllium is quite good.

3. Polished germanium substrates are useful for determination of particle thicknesses. For this work, the intensity of GeKα emission from the substrate is monitored. GeKα count rate decreases as particle thickness increases owing to increased attenuation of the electron beam by the particle.

IV. CESEMI ANALYSIS

A. Instrumentation and Computations

The details of the CESEMI instrumentation and computer programs have been described rather completely in our earlier reports and in several publications[2-5]. The important feature of this method is that entire SEM images, or several images, are recorded on digital magnetic tape with a high sensitivity grey scale (2000 possible levels). Analyses of the images are rendered by digital computer (IBM 360/67) off-line, to compute, particle by particle, the following fundamental measurements:

1) Area of each particle (μm^2)
2) Perimeter of particle (μm)
3) Semi-major axis of fitted ellipse (μm)
4) Semi-minor axis of fitted ellipse (μm)
5) Orientation of major axis (θ)
6) Particle type based on characteristic x-ray information.

From these six basic measurements, several useful parameters are derived that facilitate interpretation of results:

1) Equivalent circular diameter (μm) is calculated assuming that the particle area is located within a circle.

2) Perimeter of fitted ellipse is computed from semi-major and semi-minor axes.

3) The ratio of the particles' real perimeter divided by the computed ellipse perimeter (P/P_E) is one good measure of a particle shape complexity. Obviously, a particle with complex shape would have a greater length of perimeter than a highly rounded or smooth particle.

4) One of the most commonly used shape parameters--the aspect ratio--is the ratio of minor-to-major axis length (b/a).

5) A commonly used shape parameter is also the ratio of particle area to the square of the perimeter (A/P^2).

All these basic and derived parameters are obtained particle-by-particle. An example of these, plus the coordinate position of the particle (X and Y values) are shown in Table II.

In addition to this tabular form of data output, it is useful to graphically present the data for convenience of further study. The following plots are computer-generated for the analysis of data:

1) Probability versus equivalent circular diameter on a logarithmic scale.

2) Probability versus minor and major axes of the fitted ellipses on a logarithmic scale.

3) Probability versus merged equivalent circular diameter on a logarithmic scale.

4) Frequency versus minor/ major axis.

5) Frequency versus area/ perimeter squared.

6) Frequency versus perimeter/ ellipse perimeter.

7) Frequency versus equivalent circular diameter on a logarithmic scale.

The probability graph of the equivalent circular diameter is a logarithmic distribution to which a straight line is fitted by means of a least squares approximation. The equation of the straight line is always given in slope-intercept form with probability as ordinate and logarithmic size as abscissa. The median size (equivalent circular diameter at 50%) is also calculated. The probability graph of the major and minor axes of the fitted ellipses provides two curves with the same calculation as computed in the equivalent circular diameter. The data to both these plots represent a single magnification of a particular sample. Limits are placed on the sizes, depending on the set of magnifications used. It generally occurs that no one magnification setting is suitable to adequately measure particles over the entire range

TABLE II. EXAMPLE OF CESEMI DATA PRINTOUT FOR INDIVIDUAL PARTICLES.

AREA	E. C. DIA	PERIM	MAJOR	MINOR	THETA	ELLIP. AREA	ELLIP. PERIM	X	Y	MINOR / MAJOR	PERIM / E. PERIM	AREA / PERIM**2
12.44	3.98	9.33	0.0	0.0	0.0	0.0	0.0	14	144	0.0	0.0	0.143
7.11	3.01	9.33	0.0	0.0	0.0	0.0	0.0	16	212	0.0	0.0	0.250
1.78	1.50	1.33	0.0	0.0	0.0	0.0	0.0	21	194	0.0	0.0	1.000
39.11	7.06	24.00	49.52	1.26	11.67	172.40	193.37	23	43	0.029	0.12	0.068
1.78	1.50	1.33	0.0	0.0	0.0	0.0	0.0	24	114	0.0	0.0	1.000
10.67	3.69	8.00	0.0	0.0	0.0	0.0	0.0	24	132	0.0	0.0	0.167
1.78	1.50	1.33	0.0	0.0	0.0	0.0	0.0	25	27	0.0	0.0	1.000
24.89	5.63	16.00	3.28	1.26	21.30	12.98	15.61	25	144	0.384	1.02	0.097
3.56	2.13	2.67	0.0	0.0	0.0	0.0	0.0	26	42	0.0	0.0	0.500
17.78	4.76	12.00	0.0	0.0	0.0	0.0	0.0	26	100	0.0	0.0	0.123
1.78	1.50	1.33	0.0	0.0	0.0	0.0	0.0	26	153	0.0	0.0	1.000
1.78	1.50	1.33	0.0	0.0	0.0	0.0	0.0	26	202	0.0	0.0	1.000
5.33	2.61	4.00	0.0	0.0	0.0	0.0	0.0	27	87	0.0	0.0	0.333
1.78	1.50	1.33	0.0	0.0	0.0	0.0	0.0	27	172	0.0	0.0	.000
7.11	3.01	5.33	0.0	0.0	0.0	0.0	0.0	29	197	0.0	0.0	0.250
16.00	4.51	10.67	0.0	0.0	0.0	0.0	0.0	30	91	0.0	0.0	0.141
14.22	4.26	9.33	0.0	0.0	0.0	0.0	0.0	30	134	0.0	0.0	0.163
1.78	1.50	1.33	0.0	0.0	0.0	0.0	0.0	31	156	0.0	0.0	1.000
1.78	1.50	1.33	0.0	0.0	0.0	0.0	0.0	32	140	0.0	0.0	1.000
1.78	1.50	1.33	0.0	0.0	0.0	0.0	0.0	32	222	0.0	0.0	1.000
1.78	1.50	1.33	0.0	0.0	0.0	0.0	0.0	33	121	0.0	0.0	1.000
17.78	4.75	13.33	0.0	0.0	0.0	0.0	0.0	33	164	0.0	0.0	0.100
1.78	1.50	1.33	0.0	0.0	0.0	0.0	0.0	33	213	0.0	0.0	1.000
1.78	1.50	1.33	0.0	0.0	0.0	0.0	0.0	34	185	0.0	0.0	1.000
1.78	1.50	1.33	0.0	0.0	0.0	0.0	0.0	35	87	0.0	0.0	1.000
5.33	2.61	4.00	0.0	0.0	0.0	0.0	0.0	35	218	0.0	0.0	0.333
1.78	1.50	1.33	0.0	0.0	0.0	0.0	0.0	35	229	0.0	0.0	1.000
42.66	7.37	18.67	6.36	2.24	-36.33	30.67	21.77	36	51	0.514	0.85	0.127
1.78	1.50	1.33	0.0	0.0	0.0	0.0	0.0	36	146	0.0	0.0	1.000
8.89	3.36	6.67	0.0	0.0	0.0	0.0	0.0	37	191	0.0	0.0	0.200
35.55	6.73	16.67	4.05	2.06	-3.61	27.76	21.15	37	191	0.479	0.98	0.102
3.56	2.13	2.67	0.0	0.0	0.0	0.0	0.0	37	219	0.0	0.0	0.500
1.78	1.50	1.33	0.0	0.0	0.0	0.0	0.0	38	214	0.0	0.0	1.000
1.78	1.50	1.33	0.0	0.0	0.0	0.0	0.0	39	24	0.0	0.0	1.000
16.00	4.51	12.00	0.0	0.0	0.0	0.0	0.0	39	39	0.0	0.0	0.111
1.78	1.50	1.33	0.0	0.0	0.0	0.0	0.0	39	221	0.0	0.0	1.000
12.44	3.98	9.33	0.0	0.0	0.0	0.0	0.0	40	83	0.0	0.0	0.143
39.11	7.06	20.00	8.73	2.41	-41.42	24.93	20.09	40	226	0.629	1.00	0.098
24.89	5.63	14.67	8.61	1.35	-8.53	15.33	17.14	41	121	0.373	0.86	0.116
1.78	1.50	1.33	0.0	0.0	0.0	0.0	0.0	44	66	0.0	0.0	1.000
1.78	1.50	1.33	0.0	0.0	0.0	0.0	0.0	44	143	0.0	0.0	1.000
1.78	1.50	1.33	0.0	0.0	0.0	0.0	0.0	44	192	0.0	0.0	1.000
1.78	1.50	1.33	0.0	0.0	0.0	0.0	0.0	45	170	0.0	0.0	1.000
1.78	1.50	1.33	0.0	0.0	0.0	0.0	0.0	46	30	0.0	0.0	1.000
1.78	1.50	1.33	0.0	0.0	0.0	0.0	0.0	46	110	0.0	0.0	1.000
1.78	1.50	1.33	0.0	0.0	0.0	0.0	0.0	46	128	0.0	0.0	1.000
10.67	3.69	8.00	0.0	0.0	0.0	0.0	0.0	46	199	0.0	0.0	0.167
37.35	6.89	18.67	3.93	2.08	37.41	25.64	19.75	46	217	0.528	0.95	0.107
1.78	1.50	1.33	0.0	0.0	0.0	0.0	0.0	47	182	0.0	0.0	1.000
1.78	1.50	1.33	0.0	0.0	0.0	0.0	0.0	47	204	0.0	0.0	1.000
1.78	1.50	1.33	0.0	0.0	0.0	0.0	0.0	48	148	0.0	0.0	1.000
1.78	1.50	1.33	0.0	0.0	0.0	0.0	0.0	51	212	0.0	0.0	1.000
12.44	3.98	8.00	0.0	0.0	0.0	0.0	0.0	52	33	0.0	0.0	0.194

of importance in a given sample. Typically in this work, we have recorded data at three magnification settings: 1) 5000X, 2) 1250X and 3) 300X. In order to view results of the entire sample, a merging procedure has been developed in which the graph represents all magnifications of a sample. All data from a sample are merged together with no overlap between magnifications. The merge begins with the highest magnification recordings and descends to the lowest magnification recordings. The lower size limit is generally taken as a particle having two picture points in its area. The maximum size used from a given magnification corresponds to a value where edge-touching becomes significant. The lowest magnification will generally require no upper size cut-off. Note that the upper size limit for a given magnification becomes the lowest size limit of the next lowest magnification but the limits must meet both of the qualifications mentioned above. In this study, particles in the size range of 0.2-1.0 μm were taken from 5000X magnification, 1.0-5.0 μm from the 1250X magnification and 5.0 μm, and larger from 300X magnification.

The number counts are then weighted with respect to the set of magnifications. For example, if the set of magnifications were 2000X and 500X, a particle at 2000X would have to be weighted by a factor of 16 because the area of the 500X represents 16 times the area of 2000X. This concept is illustrated in Fig. 1.

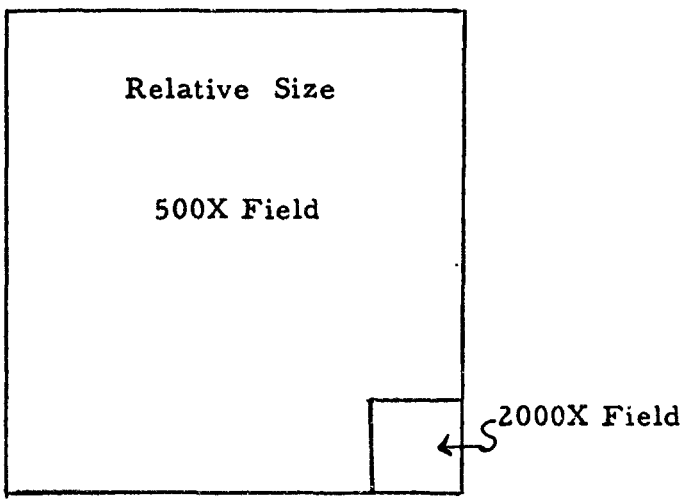

Fig. 1. Basis for weighting number-counts as a function of ratio of $(\text{magnification})^2$.

B. Analysis of the Ten Aluminas

The ten aluminas characterized by CESEMI were all recorded as follows:

Signals used:	Secondary electron
Matrix size:	256 points/line, 256 lines/frame
Number of frames:	Three at 5000X, three at 1250X and three at 300X
Tape speed:	37.5 ips at 556 bpi
Dwell time/ picture point:	180μs
Recording time/ frame:	20 sec.
Threshold level:	-6V
Signal smoothing:	25 μs time constant
Specimen current:	2.5×10^{-10} amp
Acceleration potential:	25 kev

Identification of each sample together with the computed median size and calculated slope of distribution curve are tabulated in Table III. The slope is computed by least square fit to straight line for data between 5% and 95% in the cumulative distribution

Figure 2 gives the computer-plotted size distribution curves for the 10 samples plotted on a number-count basis. Aspect ratio histograms are given in Fig. 3 . This shape complexity factor (P/P_E) histograms are plotted in Fig. 4..

Figure 5 gives the computer-plotted size distributions curves for the 10 samples plotted on a weight basis. Particle weights are computed by using the equivalent circular diameters to calculate particle volumes. A density of 3.0 gm/cm^3 was assumed for all the aluminas.

TABLE III. ALUMINA SAMPLE DESCRIPTIONS, MEDIAN SIZES AND SLOPES OF DISTRIBUTION CURVES.

Lab. Designation Alumina #	Description	Median Size(μm)	Slope
1	Norton 38-320	5.18	0.63
2	Norton 38-500	1.80	0.92
3	Norton 38-1200	0.54	0.94
4	Alcoa XA-16	0.31	2.02
5	Linde A	0.29	1.29
6	Geoscience 5μ	1.80	0.83
7	Fisher Polishing A-30.	-	-
8	Alcoa A-15 Superground	0.37	1.83
9	Alcoa A-17 Reactive	0.42	1.95
10	Meller Alumina Lot #42	0.46	1.88
11	Meller Alumina Lot #48	0.31	1.30

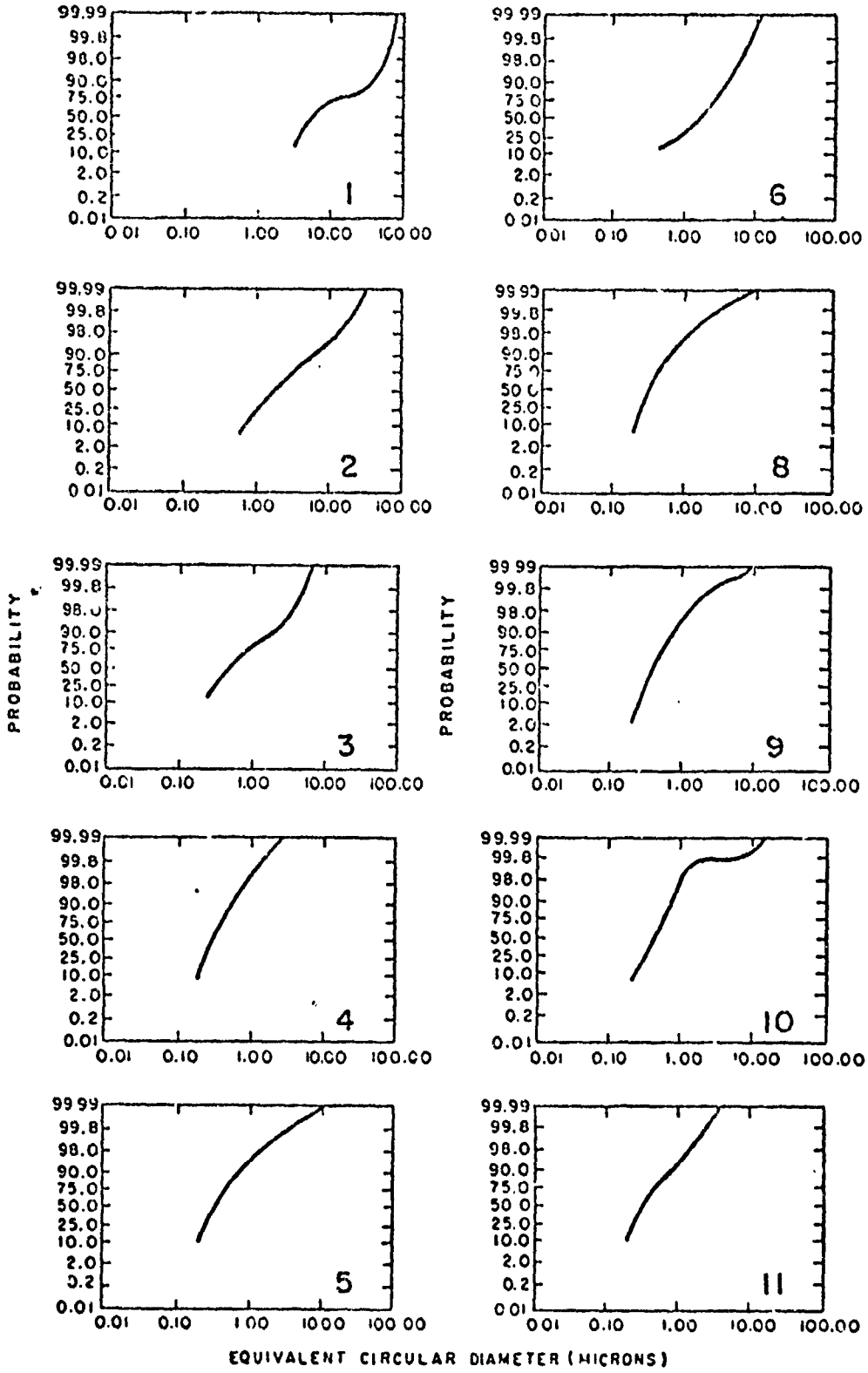

Fig. 2. Computer-plotted curves of probability versus logarithmic size (number-count basis) for the ten aluminas.

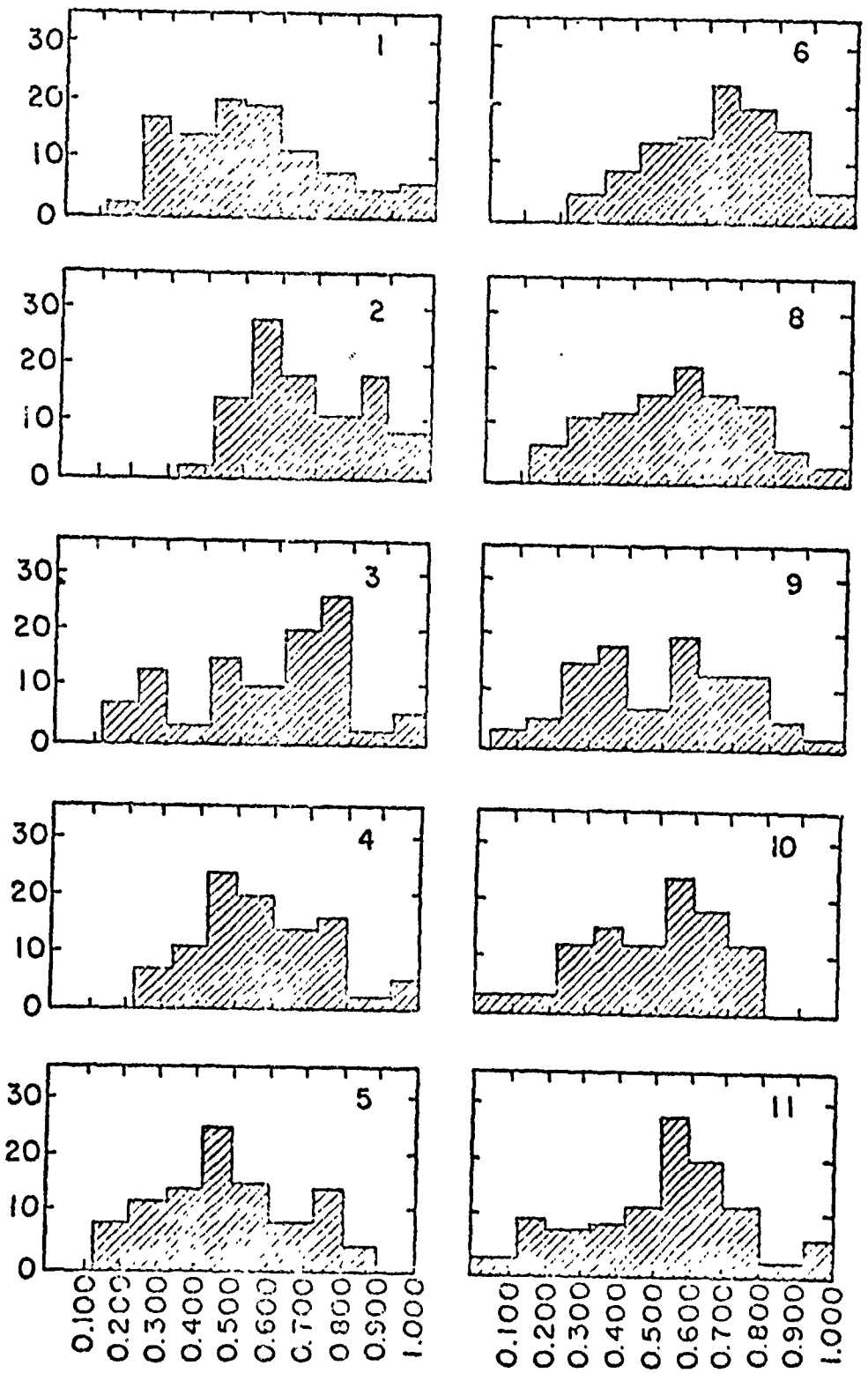

Fig. 3. Computer-plotted histograms of the aspect ratios (b/a) for the ten aluminas.

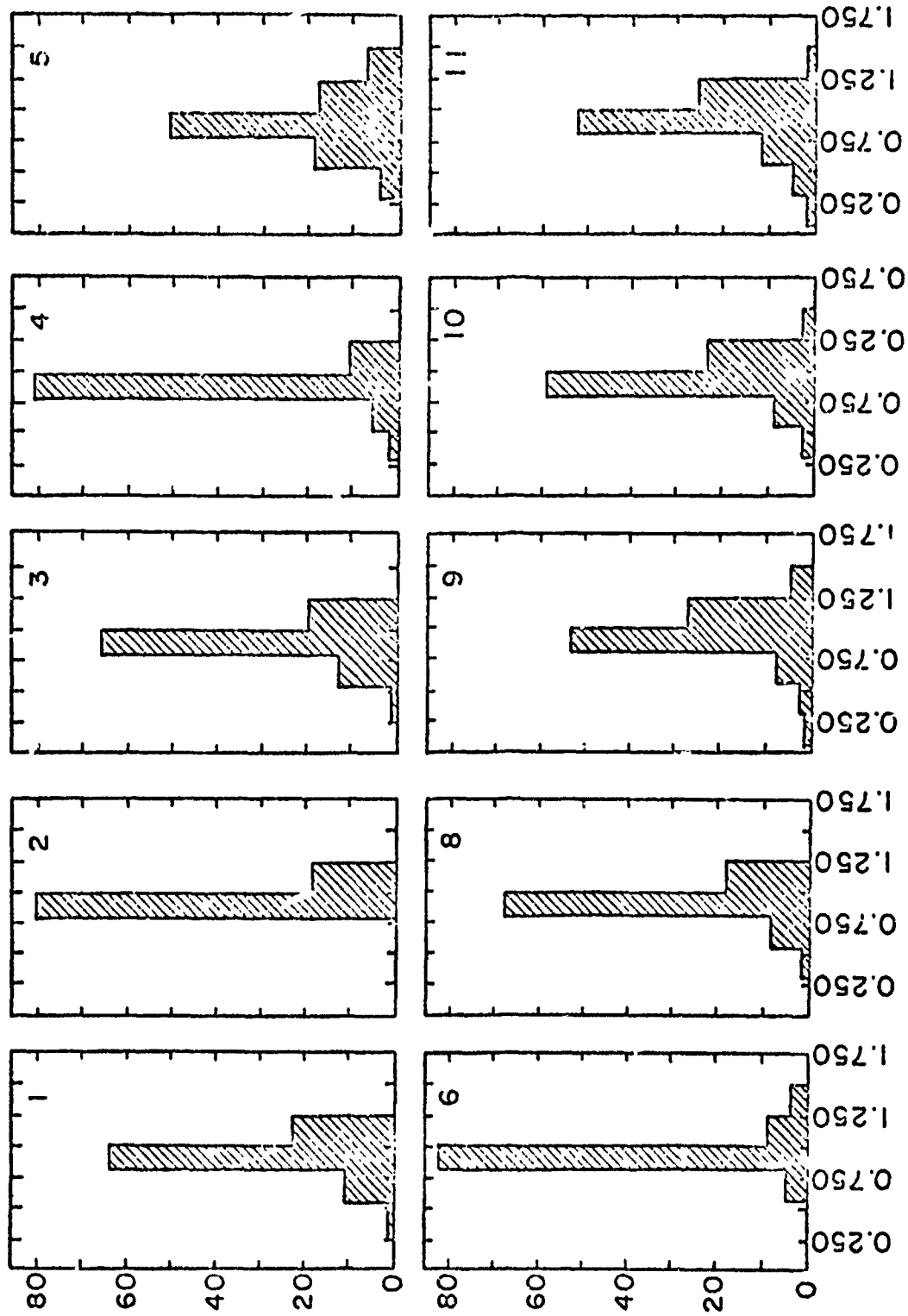

Fig. 4. Computer-plotted histograms for the shape complexity factor P/PE for the ten aluminas.

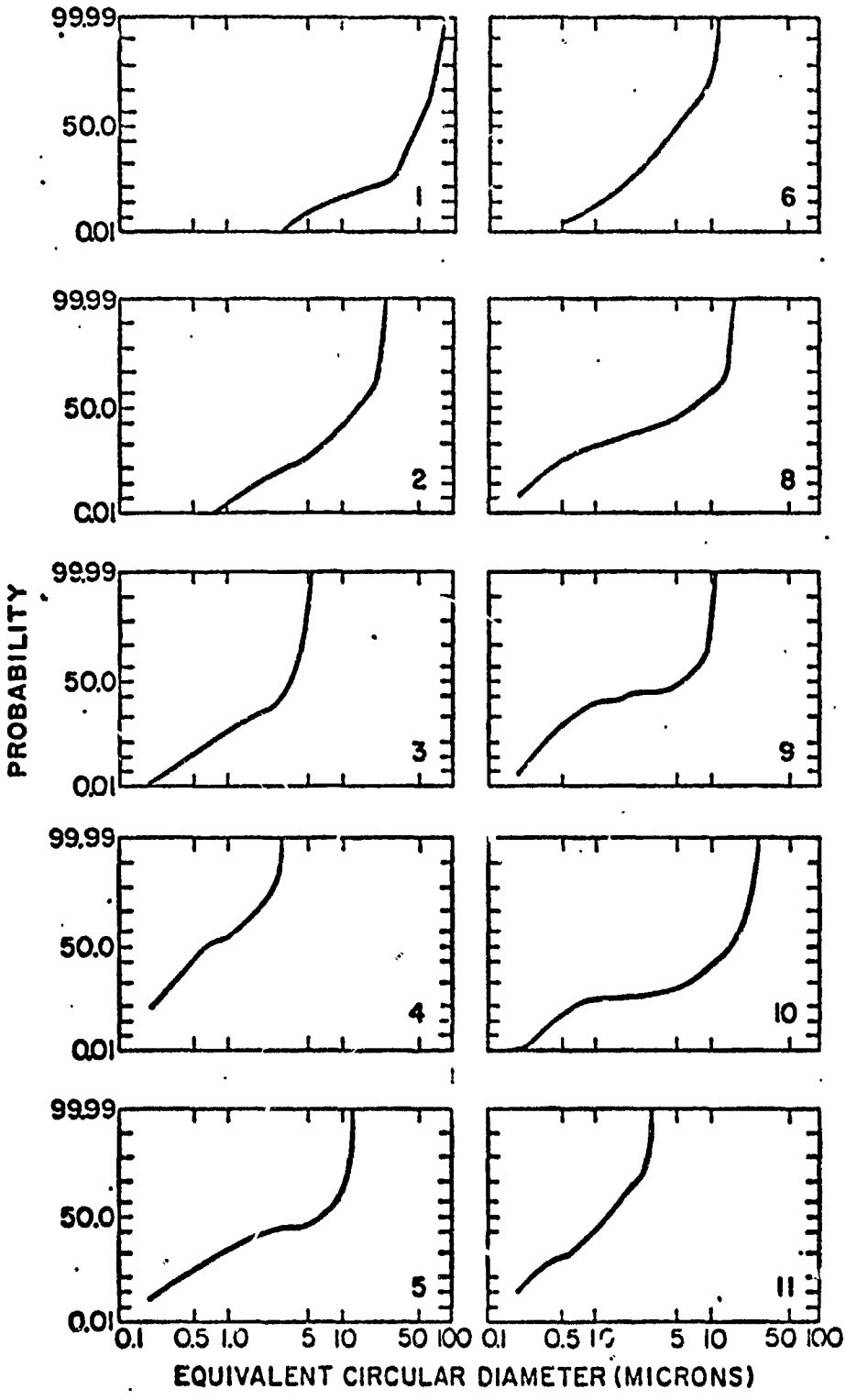

Fig. 5. Computer-plotted curves of probability versus logarithmic size (cumulative weight basis) for the ten aluminas.

V. SIMPLE METHODS FOR AUTOMATIC QUANTITATIVE ANALYSIS OF SEM AND PROBE IMAGES

Techniques for quantitative image evaluation range from sophisticated computer analyses such as by CESEMI and dedicated image analyzing computers, to the tedious manual techniques. The purpose of this chapter is to describe an intermediate approach that utilizes, to a great extent, the electronic read-out systems associated with most microprobes and SEMs. In this work quantitative image analysis data are accumulated on conventional scalers or alternatively in a multichannel analyzer and read-out on teletype. Techniques for converting these data to particle size distributions, pore size distributions, percent of phase, specific surface area, etc. have been applied to these basic quantitative image measurements. Results for the 11 aluminas will be presented and compared with the full CESEMI results described in Chapter IV.

A. Instrumentation

The method is based on selecting a signal threshold value to distinguish a selected phase. Various signals, such as secondary electron, electron back-scatter or cathodoluminescence, are analog signals while the characteristic x-ray signals, that are normally digital, may be converted to analog form. Having an analog signal, an analog comparator is used for making the decision as to when the electron beam is on or off the selected phase. The image is generated by scanning with a digitally-controlled sweep system such that the image is broken down into a matrix of known number of points. Thus the picture is generated point-after-point, and this is used for simultaneous analysis of each such point while the picture is being formed. The measurement of on-to-off ratio or, in other words, the selected phase to background ratio does not even require a square matrix of points. A digitally-controlled sweep system has a great advantage in comparison with other systems in that it is easier to vary sweep speed for a given size of matrix.

This enables one to select the optimum acquisition speed at acceptable signal-to-noise ratio. Most of the special purpose image analyzing computers and hardware systems have serious limitations because they usually operate at the fixed TV scan speed which is not acceptable in most SEM applications because of inherent low signal-to-noise ratio. In fact, many of the x-ray mapping techniques require a scanning speed on the order of 100 ms per line or more, depending on excitation voltage, incident beam intensity and concentration of the particular element in the sample. A great deal of freedom in deflection speed selection thus allows one to achieve acceptable signal-to-noise ratios even under rather unfavorable conditions.

1. Basic Logic Circuits

To fully understand the principles of this approach to image analysis, one must understand at least a few basic electronic logic symbols and their functions:

i. Analog Comparator is not a pure logic unit; it is an interface between analog and digital units. The input is an analog signal compared with a fixed reference. An ideal analog comparator has only two output states called true or false: true if the compared analog input is greater or more positive than the selected reference value, and false if the input is below or less positive than the reference. The true and false conditions may be expressed simply as one and zero corresponding to one for true (+5V) and zero for false (0V). To designate the analog comparator, a symbol, similar to a differential amplifier, is used because it is essentially a nonlinear high gain differential amplifier with output clamped to standard logic level.

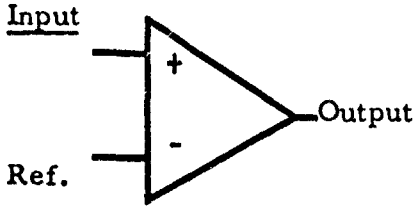

EXAMPLE

Input	Ref.	Output	Logic
+10V	0V	1	True
+0.01V	0V	1	True
-0.01V	0V	0	False
-10V	0V	0	False

ii. The AND-Gate consists of two inputs, 'A' and 'B', and one output. The truth table fully describes the function and may be read as follows:

A	B	Out
0	0	0
1	0	0
0	1	0
1	1	1

The output will be true (one) only while both inputs are true (one). Every other combination at inputs gives zero output.

iii. The NAND-Gate is an AND-Gate with an inverter on the output giving complementary output to an AND-Gate:

A	B	Out
0	0	1
0	1	1
1	0	1
1	1	0

This gate has much more general application; therefore, it is preferably used in these circuits.

iv. "On-Phase" - "Off-Phase" Counting. A typical function of an AND-Gate, giving true output, requires both inputs to be true. Input A is supplied with positive clock pulses that are used to drive the digitally-controlled sweep system. This gives one pulse per picture point of the image. These pulses will appear on the output of the AND-Gate only if the input B is true. Input B is supplied by the signal from the comparator which is true only if the beam happens to be on the selected phase or, in other words, the signal is above the set threshold value. All points giving true output from the comparator will enable the AND-Gate and may be counted by a conventional pulse counter directly connected to the output of the AND-Gate. In Fig. 6, a toggle switch symbol

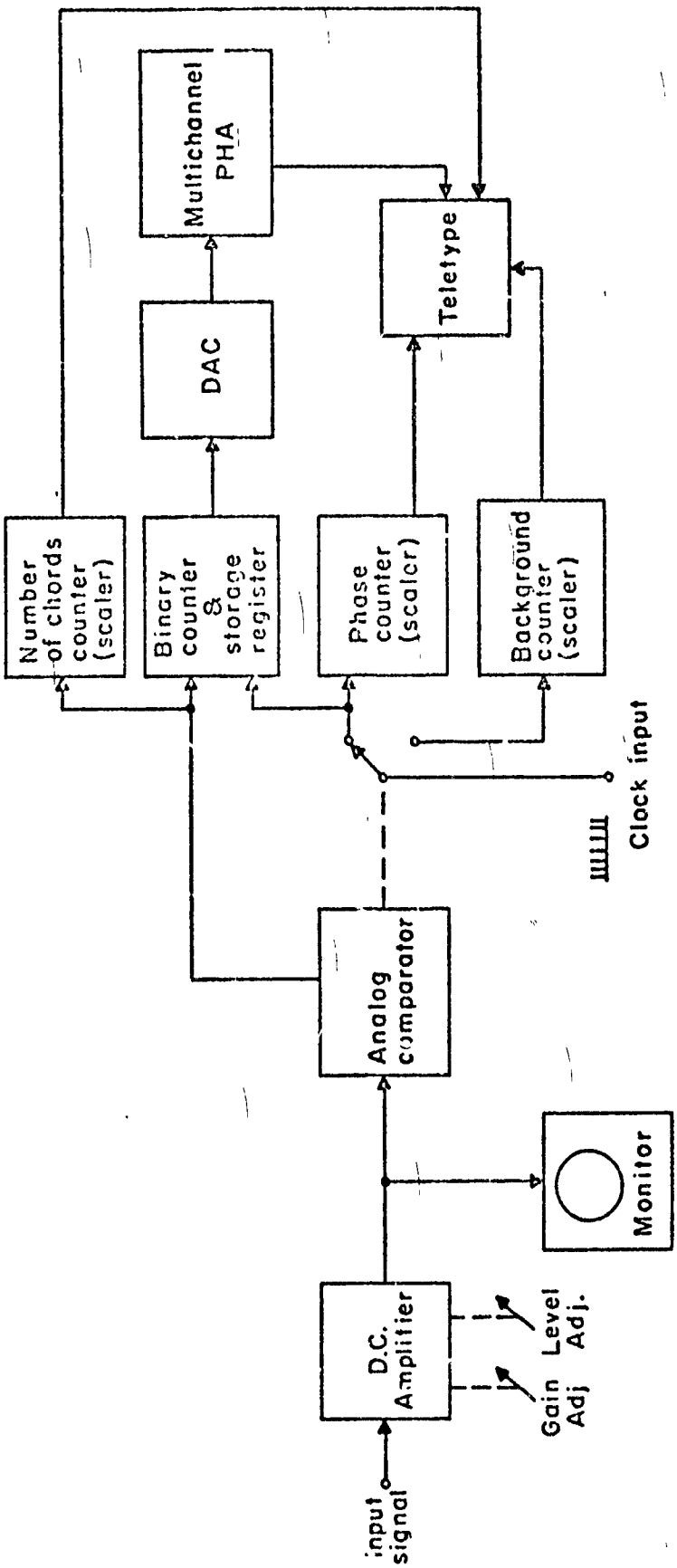

Fig. 6. Block diagram of phase integrator and chord length analyzer.

is used to illustrate the switching of clock pulses from the "on-phase" counter to "off-phase". Figure 7 is a timing diagram showing that when the electron beam is "on-phase", the clock pulses are switched from the "off-phase" counter to the "on-phase" counter.

The simple AND-Gate and comparator in connection with a counter give directly the number of points on the selected phase of the image. In the case of the digitally-controlled sweep, the total number of picture points is known; thus the ratio of "on" points to total number of points multiplied by 100% gives directly the selected phase percentage with very high precision. The repetability of such measurements is better than one percent. The accuracy, however, is essentially limited by the SEM itself because usually the distortion, non-linearity and instability of the deflection system is on the order of 2-3%.

The analog signal applied to the input of a comparator yields a standard logic output--true or false--as a result of the comparison with the critical or threshold level. The standard logic level (output of the analog comparator) directly controlls two of the NAND-Gates (top and bottom) in Fig. 8. The lower NAND-Gate functions also as an inverter and controls the middle NAND-Gate so that it passes clock pulses when "off-phase". Each of these gates has an extra input tied together as "ENABLE" input controlled by the SEM to insure an analysis of a single frame or picture per measurement. This signal may be derived from the blanking level of the CRT or by special start-stop circuit synchronized with the scanning system. The third input to the NAND-Gates is obviously the clock input giving output pulses on either the "on-phase" output or the "off-phase" output with the assumption that ENABLE is kept true.

v. Number of Chords. A chord is defined as an uninterrupted segment of raster line "on-phase". The number of chords, sometimes called crossings, may be obtained by counting the leading edges of comparator output (see Fig. 7). However, the real condition is not that simple: The analog signal is not always as smooth as in the Figure. But, even more important, an intermediate condition, where

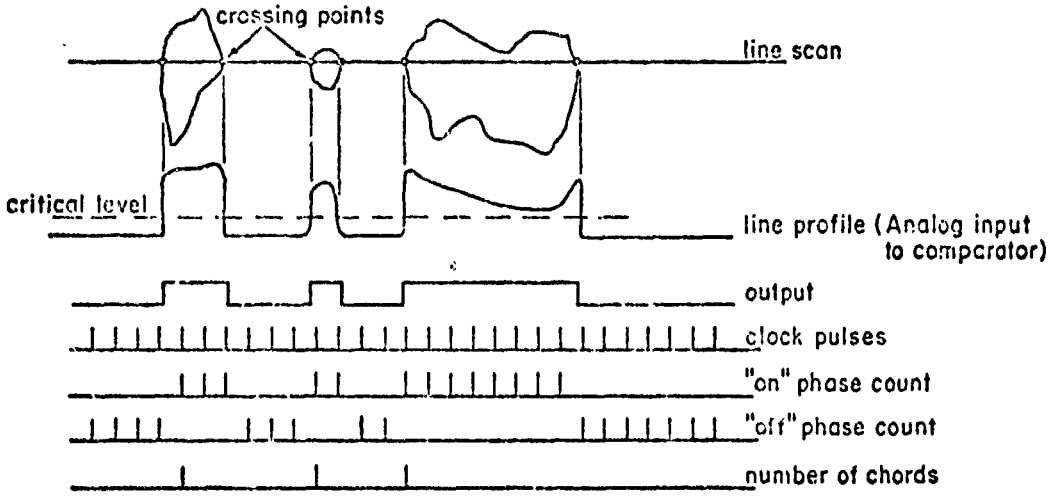

Fig. 7. Timing diagram for phase integrator.

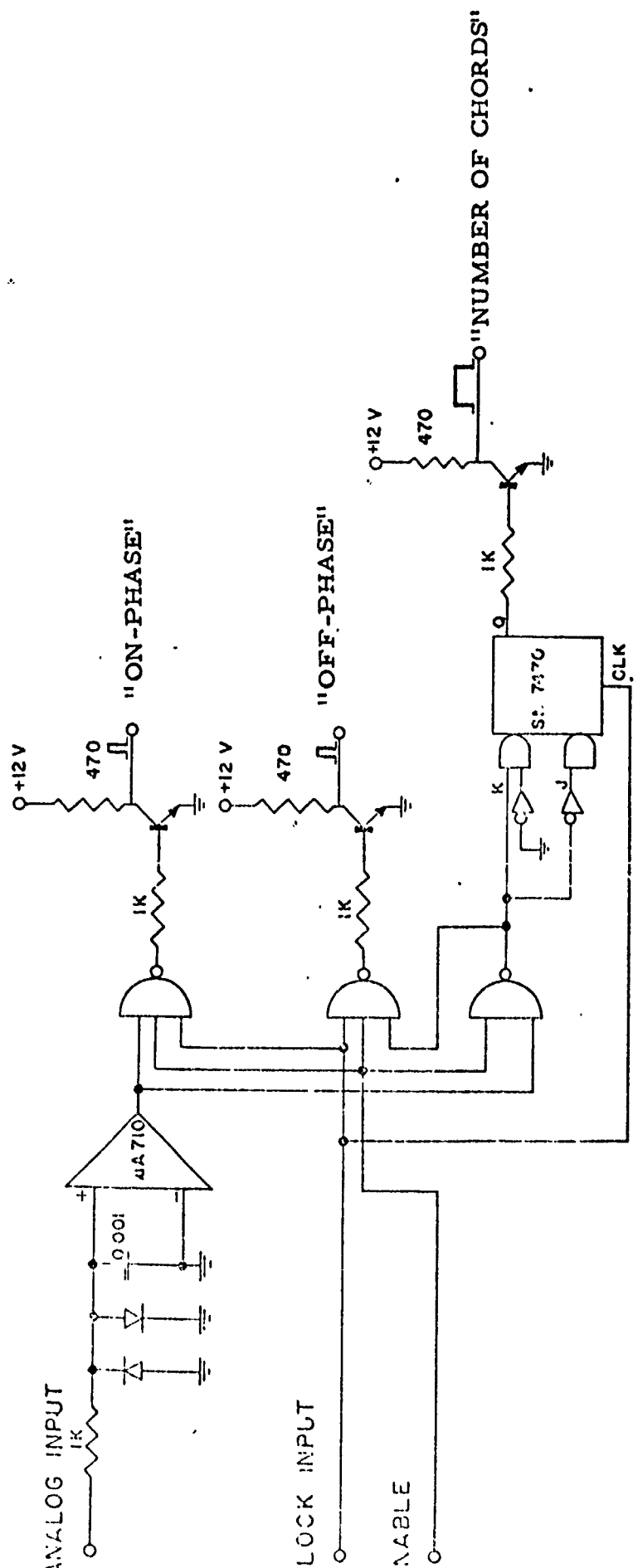

Fig. 8. Schematic diagram for comparator.

a picture point happens to yield a threshold value may be encountered. In such a case, the smallest instability of either position or brightness (always both are involved) may cause several changes in the state of output of the analog comparator; thus, a counter directly connected to the comparator output would register several leading edges and thereby, incorrectly, several chords. This problem was solved by using a clocked Flip-Flop, a circuit which transfers its input to output only once per single clock pulse. Clock pulses similar as in previous cases are derived from digitally-controlled sweep system such that every pulse corresponds to just one point of the matrix.

Figure 8 illustrates the switching of "on-phase" and "off-phase counts into two counters. Also shown are the Flip-Flop circuit for the "Number of Chords" counter and the pulse amplifiers. All three signals on the output of appropriate gate or Flip-Flop with standard level of 0-5V were not suitable to drive the counters used for this study. The signal had to be amplified to +10V.

2. Derived Parameters

From "on-phase", "off-phase" and "Number of Chords" count, together with known magnification and picture point density, one can derive a series of parameters for the quantitative description of a phase without a tedious measurement and tabulations. The following parameters may be obtained

P_p = Point fraction of phase = $\frac{\text{"on-phase"}}{\text{"on-phase"+"off-phase"}} = \frac{\text{"on-phase" Count}}{\text{Total Count}}$

$P_p = L_L = A_A = V_V$

L_L = Line fraction of phase

A_A = Area fraction of phase

V_V = Volume fraction of phase

% = Percentage of phase = $P_p \times 100\%$

$\bar{L}$ = Average chord length = $\frac{\text{"on-phase"}}{\text{"Number of Chords"}} \times C\ (\mu m)$

Where C = Real distance between two closest horizontal picture points on the specimen for the 10 x 10 cm screen of CRT and required parameters in μm

$$C = \frac{10^5}{\text{Magnification} \times \text{Number of Points/Line}} \ (\mu m/\text{point})$$

N_L = Number of chords/unit length = $\frac{\text{Number of Chords}}{(\text{"on-phase"} + \text{"off-phase"}) \times C}$ (μm^{-1})

S_V = Surface area/unit volume $\doteq 2N_L$ (μm^{-1})

SP = Average center-to-center spacing = $\frac{1}{N_L}$ (μm)

γ = Average edge-to-edge spacing = $\frac{1 - V_V}{N_L}$ (μm)

Figure 9 illustrates analysis of pores (considered as a phase) of $BaTiO_3$ capacitor. All parameters are derived from "On Pore", "Off Pore" and "Number of Chords" information read out from appropriate scaler.

Characteristic x-rays may be used to distinguish a given phase but because the signal consists of pulses, an integrator of proper sampling period must be used to convert the pulses to an analog signal acceptable by the analog comparator. A specially designed synchronous ratemeter has been designed and built. It consists of a fast digital to analog converter operating synchronously with the digital sweep, thereby converting x-ray count rate into an analog signal at each picture point. Unlike the usual R. C. ratemeter circuit, the synchronous ratemeter has no decay constant. Having the analog signal again, the analysis is exactly the same as in the above cases. The analog signal may be used, also, for brightness modulation in x-rays mapping techniques.

Other analog signals such as cathodoluminescence or electron backscatter may be used for unambiguous phase identification.

3. Method for Generating Chord Length Distributions

Additional information about a characterized phase may be obtained by studying the distribution of chord lengths. Looking back on

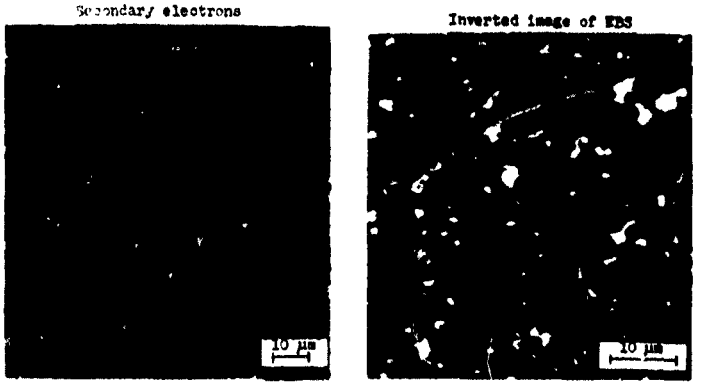

SAMPLE: $BaTiO_3$ AP.

SCALER	ON!PORE	OFF!PORE	No.of CHORDS
COUNT	[illegible],442	981,305	4,284

V_V= .0625 S_V= .168/ μm

PORE= 6.25% SP= 11.9 μm

$\bar{L}$ = .745 μm/CHORD λ = 11.16 μm

Reproduced from best available copy.

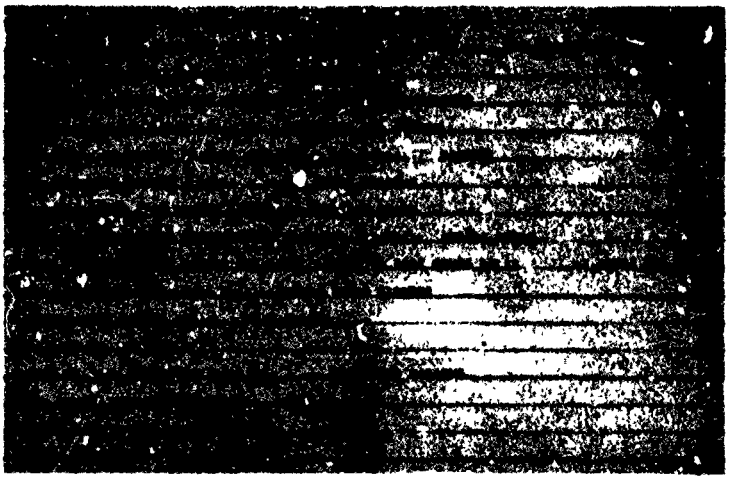

Fig. 9. Example of pore analysis using simple outputs.

Fig. 7, the timing diagram shows that the "on-phase" count contains additional information about a chord, namely its length. The first chord length of Fig. 7 is three points long; the second, two and the third is eight points long. This information could not be obtained in the three-scale method because there was no way to register the spectrum of chord lengths.

In order to obtain a distribution of chord lengths, electronic registers must be set up to store count information; thus, for every chord size interval there must be a register. Such storage was achieved by modifying a Northern NS 600 Series 512 channel multichannel pulse height analyzer.

A standard multi-channel pulse height analyzer accepts pulses of height in the range of 0-10V, and of several microseconds duration. Two normalized logic signals are available from the analog comparator for use in the chord length to pulse height conversion: 1) the level output from comparator of duration proportional to the particular chord length and 2) clock pulses, which track the position of the electron beam on the sample. Figure 10 illustrates the process of conversion. The "Number of Chords" signal serves two functions: a) to open the gate for clock pulses (see the truth table for "NAND-Gate"), and b) to disable the "One-Shot A" from strobing the counter or triggering the "One-Shot B".

The timing diagram shows an example of conversion of a three picture point chord to a pulse of proportional height. In this example, the gate is enabled by the "Number of Chords" signal, and clock pulses are counted by an eight-bit binary counter. The positive edge of "Number of Chords" signal disables "One-Shot A" and "B". The negative edge, on the end of the chord, triggers the "One-Shot A"; thus, the strobe transfers the accumulated count from the counter to the DAC, and a voltage proportional to that count appears on the output of the digital to analog converter. The strobe pulse of duration 10μs, triggers the "One-Shot B" by its negative edge, causing a reset of the counter and re-triggering of "One-Shot A". The "A" circuit strobes the counter again, thus transferring the zero count to the DAC and thereby on the output appears a zero volt analog signal. The resulting output signal is a pulse of fixed duration, about 10μs, and a height proportional to

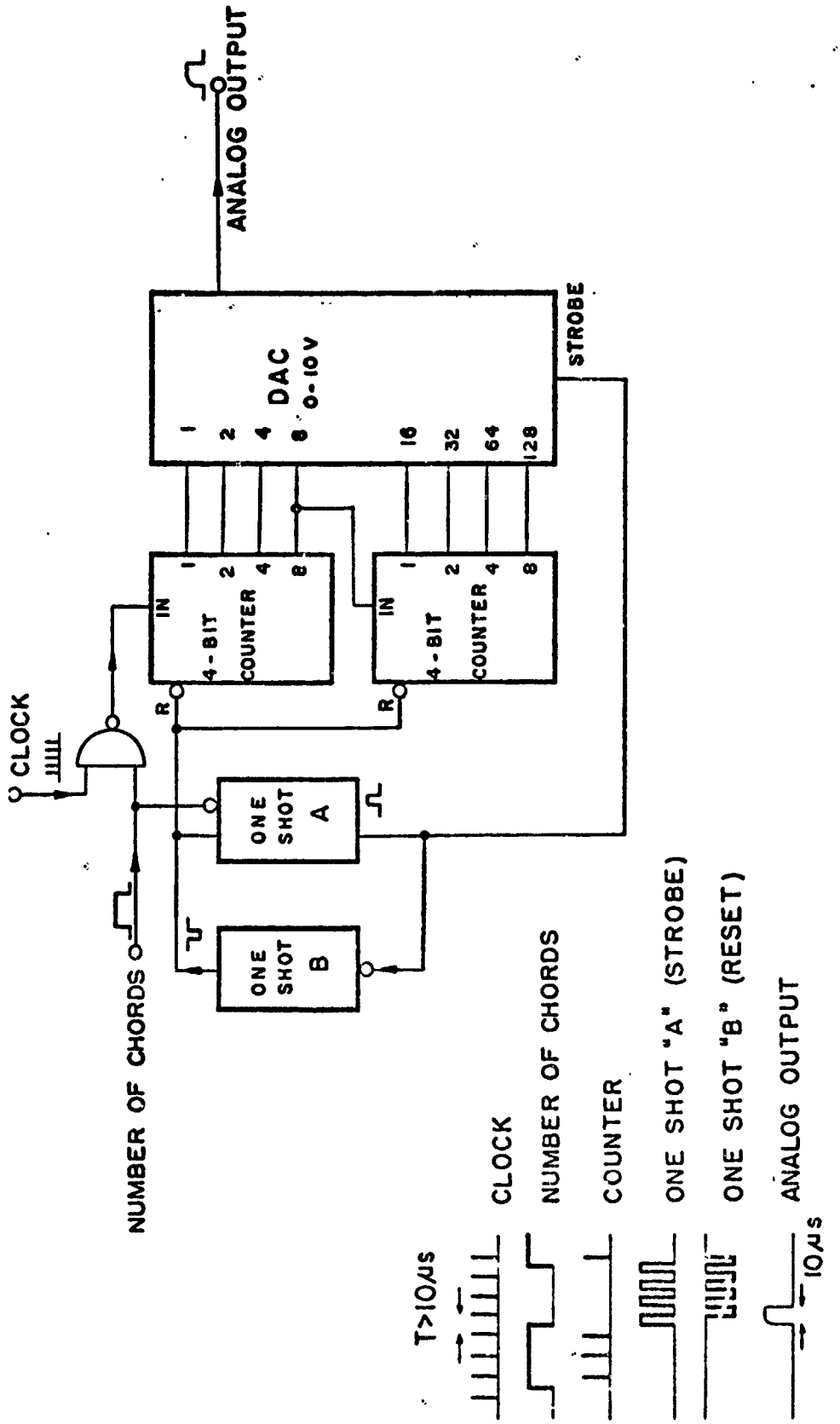

Fig. 10. Conversion of number of picture points in chord to pulse of proportional height.

chord length. The two "One-Shots" will oscillate by triggering each other continuously, re-setting the counter and strobing the zero to output of the DAC unless a new chord appears on the input-gate. For practical analysis, however, two limitations of the converter must be considered. The maximum chord length is limited by size of the counter to 256 points and the output of 0-10V must be attenuated to exactly match the input of a multichannel PHA--usually around 0-8V. This method does not require any modifications of used multichannel analyzer.

Alternatively, the direct access method eliminates a need for the above converter, attenuator and the only limitation for chord length size is the number of channels available in multichannel PHA. However, the interface in this case is more complex and requires a modification of the multichannel analyzer. This second method may be considered superior to conversion because it does simplify operation and is more economical and guarantees a storage of a chord, n-points long into n-th channel, which cannot always be guaranteed in the previous method.

Figure 11 illustrates two distributions taken from the display of the multichannel analyzer for # alumina-A301 particles and in polished cross section of $BaTiO_3$. The pore distribution indicates a peak value around 0.5μm.

4. Parameters Derived from Chord Length Distributions.

Two coefficients must be established before attempting to derive a useful measurement from the distribution:

1. P = Total number of picture points sampled (number of horizontal points per line times number of lines times number of frames).

2. C = Calibration factor. For a 10 x 10 cm CRT screen the calibration factor becomes:

$$\frac{10^5}{\text{Magnification} \times \text{Number of Points/ Line}} \quad (\mu m/\text{ Point})$$

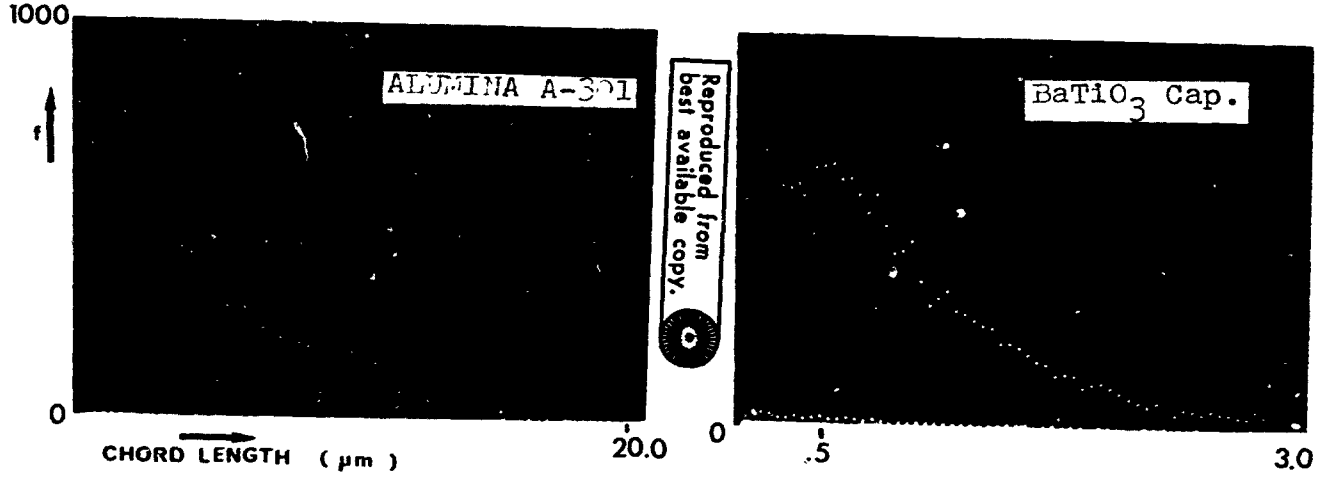

Fig. 11. Example of chord length distributions for an alumina sample and pores in polished section of $BaTiO_3$ capacitor.

Then the derived parameters applicable to polished sections are:

P_p = point fraction of "on" points $P_p = \frac{\sum_{1}^{n} f_i L_i}{P}$

$P_p = L_L = A_A = V_v$

% = percentage of phase = $P_p \times 100\%$

n = number of different chord sizes (or number of channels used)

f_i = cumulative frequency of i-th size

$\bar{L}$ = average chord length $\bar{L} = \frac{\Sigma f_i L_i \, C \, (\mu m)}{\Sigma f_i}$

N_L = number of features per unit length of line = $\frac{\Sigma f_i}{P.C.} \, (\mu m)$

S_v = surface area/ unit test volume $\doteq 2N_L \, (\mu^{-1})$

λ = edge-to-edge mean free path = $\frac{1 - V_v}{N_L} \, (\mu m)$

SP = center-to-center spacing = $\frac{1}{N_L} \, (\mu m)$

Presently, the analysis is done by obtaining chord length distribution on multichannel PHA (Northern Scientific, NS-600) from SEM model JSM1, punching the distribution data on paper tape, adding the two necessary coefficients P, C and using the tape or data input for the PDP-11. A short program yields all derived parameters plus a condensed distribution of chords; thus, no manual measurements or calculations are involved.

B. Linear Analysis for Eleven Aluminas

The eleven aluminas shown in Table III were analyzed by lineal analysis, using the following recording conditions:

Signal used:	Secondary electron
Matrix size:	1024 points/ line, and 256 lines/ frame
Number of frames:	Five at 2000X, and five at 200X
Dwell time/ picture point:	0.25 ms
Recording time:	60 sec. / frame
Threshold level:	0 volts
Signal smoothing:	0.25 ms
Specimen current:	2.5×10^{-10} amp
Acceleration potential:	25 kev
Storage:	Multichannel analyzer (128 or 256 channels used with direct access interface.

As in the case of CESEMI recordings, it is found that more than one magnification is required to adequately cover the typical range of particle sizes. However, since the picture point density is higher than for the CESEMI recordings (1024 vs. 256 points per line), it was found that just two magnifications were sufficient. The data from the two magnifications are merged as follows to form one distribution.

Channels two through 99 were used from the 2000X magnification data. Counts in these channels were multiplied by 10 to adjust for relative lengths of sample line at the two magnifications. Channels 10 and up were used from the 200X magnification. The calibration factors are: 0.0488μm/ picture point at 2000X and 0.488μm/ picture point at 200X.

The merged chord length distributions were converted to particle size distribution by the function:

$$t_n = \sqrt{D_m^2 - ((n-1)x2)^2}$$

where:

t_n = length of nth chord

D_m = maximum diameter (assuming spherical shape)

n = number of chords of length t_n

Results for the eleven aluminas are plotted in Fig. 12.

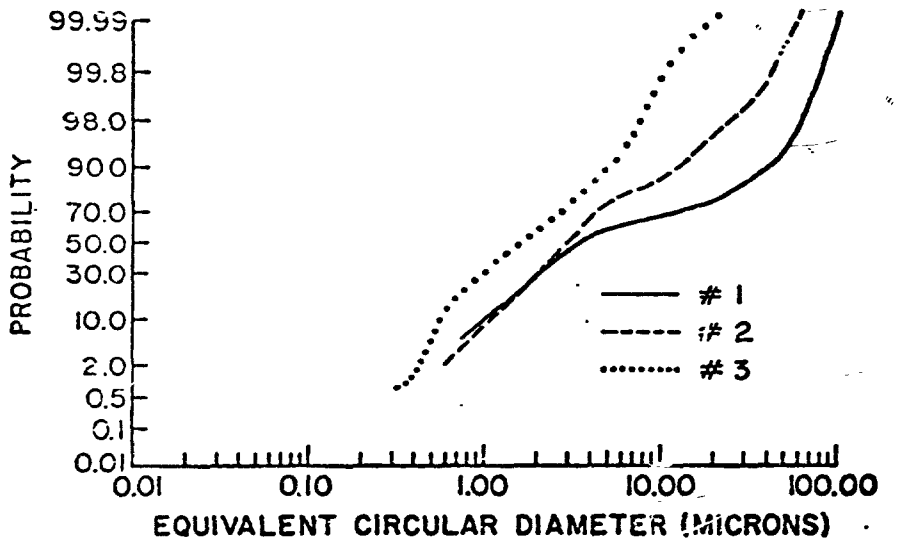

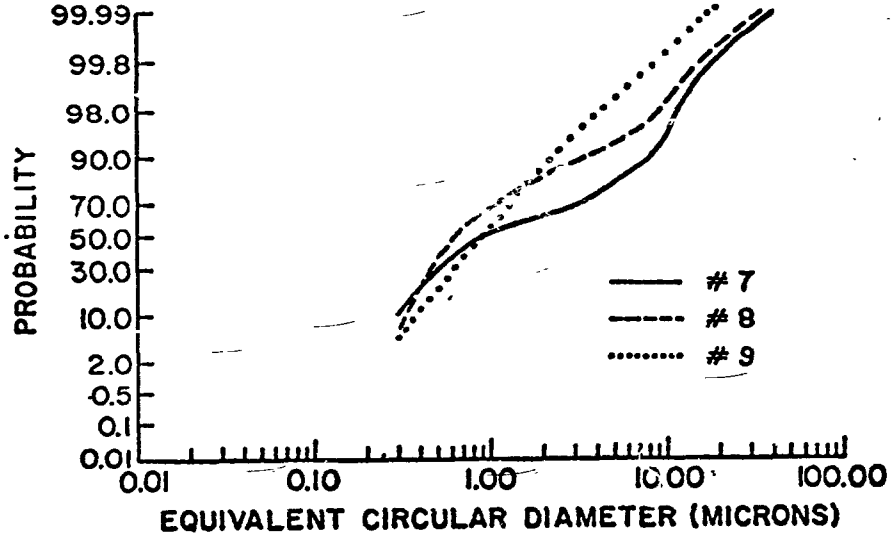

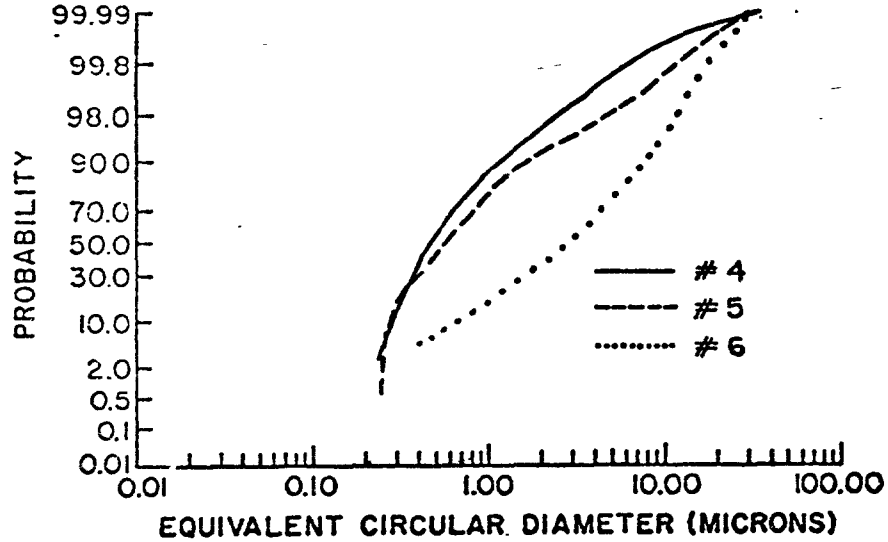

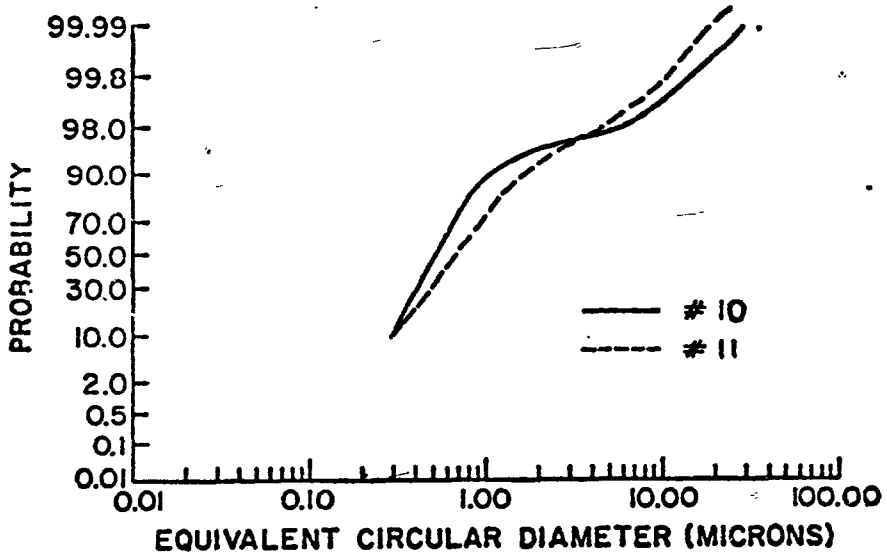

Fig. 12. Particle size distributions for 11 aluminas obtained from chord-length distributions.

VI. DISCUSSION OF RESULTS

Data from the three sets of size distributions (shown in Figs. 2, 5 and 12) are summarized in Table IV. Tabulated values are for the 10% cumulative (percent smaller than), median and 90% cumulative. A few of the 10% value are not listed for the CESEMI number count data since they could not be obtained without extrapolating the curves.

The CESEMI number count distributionsare the most accurate of the three as the fewest number of assumptions are involved in their calculation. The main assumption is that the particles are randomly oriented on the substrate. CESEMI weight distribution curves (Fig. 5) are computed on the basis of having assumed that volume can be computed from equivalent circular diameters. A density of 3.0 gm/cm^3 was assumed for the aluminas. The lineal analysis number count distribution curves inherently involve the greatest number of limiting assumptions, the most important being the assumption of particle shape which is the basis of conversion from chord length distribution to number versus size distribution.

The selection of aluminas included in this study represent a wide range of particle sizes, size distributions and methods of manufacture.

Four types of size distributions are observed in Fig. 2:

1. Several samples have strongly bimodul size distributions:
   a) Norton 38-320 - (1)
   b) Norton 38-1200 - (3)
   c) Meller Lot #42 - (10)

2. Only three samples yield essentially log normal size distribution:
   a) Norton 38-500 - (2)
   b) Alcoa XA-16 - (4)
   c) Meller Lot #48 - (11)

3. Three samples are quite similar with distributions skewed

TABLE IV. SUMMARY OF PARTICLE SIZE DISTRIBUTION DATA

LAB. Alumina #	DESCRIPTION	CESEMI NUMBER Distribution			CESEMI WEIGHT Distribution			LINEAL ANALYSIS Number Distribution		
		10%	Median	90%	10%	Median	90%	10%	Median	90%
1	Norton 38-320	-	5.18	42.00	31.80	48.50	65.00	0.99	3.60	41.00
2	Norton 38-500	0.70	1.80	7.00	7.40	15.70	21.70	1.16	3.10	16.00
3	Norton 38-1200	-	0.54	1.80	1.84	3.60	4.55	0.58	1.75	4.60
4	Alcoa XA-16	0.21	0.31	0.56	0.33	0.59	1.78	0.29	0.48	1.19
5	Linde A	-	0.29	0.86	0.90	6.50	11.40	0.27	0.56	1.80
6	Geoscience 5μ	-	1.80	4.70	3.28	5.29	8.90	0.71	2.99	8.10
7	Fisher Polishing A-301	-	-	-	-	-	-	0.31	0.95	8.90
8	Alcoa A-15 Superground	0.22	0.37	0.70	1.63	7.80	14.10	0.34	0.63	3.80
9	Alcoa A-17 Reactive	0.27	0.42	0.85	0.69	6.15	9.90	0.39	0.92	2.40
10	Meller Alumina Lot #42	0.25	0.46	0.78	8.00	21.90	26.80	0.32	0.54	1.35
11	Meller Alumina Lot #48	0.19	0.31	0.88	0.62	1.34	2.58	0.32	0.69	1.75

toward the small particle size:

a) Linde A - (5)
b) AlcoaA-15 Superground - (8)
c) Alcoa A-17 Reactive - (9)

Linde A and A-15 are nearly identical. It is important to bear in mind that these results are for samples that are not ball-milled.

It was encouraging to observe the similarity in the shapes of number distribution curves for the full CESEMI (Fig. 2) and lineal analysis (Fig. 12).

The lineal analysis results find median and 90% size values that are two to three times larger than for the full CESEMI. This is a direct result of the circular shape assumption used in the lineal analysis. The one exception is for Norton 38-320 (1) which yielded quite comparable results by the two techniques.

REFERENCES

1) Thaulow, N. and E. W. White, "General Method for Dispersing and Disaggregating Particulate Samples for Quantitative SEM and Optical Microscope Studies," Technical Report No. 5, ONR Project No. NR-032-502; November, 1971 (In press, Powder Technology.)

2) White, E. W., H. A. McKinstry, G. G. Johnson, Jr., "Computer Processing of SEM Images," Proc. Scanning Electron Microscopy Symp., 95-103 (1968), IITRI, Chicago, Illinois.

3) McMillan, R. E., G. G. Johnson, Jr., E. W. White, "Computer Processing of Binary Maps of SEM Images," Proc. Scanning Electron Microscopy Symp., 439-444 (1969), Editor: O. Johari; IITRI, Chicago, Illinois.

4) Matson, W. L., H. A. McKinstry, G. G. Johnson, Jr., E. W. White, R. E. McMillan, "Computer Processing of SEM Images by Contour Analyses," Pattern Recognition 2 303-312 (1970).

5) White, E. W., K. Mayberry and G. G. Johnson, Jr., "Computer Analysis of Multi-Channel SEM and X-ray Images From Fine Particles," Technical Report No. 3; ONR Project No. NR-032-502; 22 December 1970 (In press, Pattern Recognition.)